JACS
JOURNAL OF THE AMERICAN CHEMICAL SOCIETY

Communication

pubs.acs.org/JACS

Noncovalent Intermediate of Thymidylate Synthase: Fact or Fiction?

Svetlana A. Kholodar and Amnon Kohen*

Department of Chemistry, The University of Iowa, Iowa City, Iowa 52242-1727, United States

Supporting Information

ABSTRACT: Thymidylate synthase is an attractive target for antibiotic and anticancer drugs due to its essential role in the *de novo* biosynthesis of the DNA nucleotide thymine. The enzymatic reaction is initiated by a nucleophilic activation of the substrate via formation of a covalent bond to an active site cysteine. The traditionally accepted mechanism is then followed by a series of covalently bound intermediates, where that bond is only cleaved upon product release. Recent computational and experimental studies suggest that the covalent bond between the protein and substrate is actually quite labile. Importantly, these findings predict the existence of a noncovalently bound bisubstrate intermediate, not previously anticipated, which could be the target of a novel class of drugs inhibiting DNA biosynthesis. Here we report the synthesis of the proposed intermediate and findings supporting its chemical and kinetic competence. These findings substantiate the predicted nontraditional mechanism and the potential of this intermediate as a new drug lead.

Thymidylate synthase (TSase) is a key enzyme in cell proliferation, as it catalyzes a reaction essential for DNA replication, a reductive methylation of 2′-deoxyuridine-5′-monophosphate (dUMP) to form 2′-deoxythymidine-5′-monophosphate (dTMP) using the cosubstrate N5,N10-methylene-5,6,7,8-tetrahydrofolate (CH_2H_4F).[1] Accordingly, targeting TSase remains one of the most successful approaches in cancer treatment[2] and one of the prospective approaches in antibacterial chemotherapy.[3] Structural analogs of dUMP (e.g., fluoropyrimidines) and CH_2H_4F (e.g., antifolates) are well-established drugs targeting TSase. Despite many therapeutic advantages, these agents lead to toxicity and development of acquired resistance in cells.[4] Consequently, alternative strategies to improve selectivity and find new classes of TSase inhibitors are pursued.[4−6] In this respect, mechanistic studies of TSase-catalyzed reaction can provide invaluable insights.

The TSase-catalyzed reaction involves the consecutive donations of a methylene and a hydride from cosubstrate CH_2H_4F to dUMP. The traditionally accepted mechanism[1] has been recently scrutinized using computational[7−9] and experimental[10,11] approaches. While the role of an enzymatic cysteine in activating the substrate (Scheme 1, step 1) and attacking the methylene (step 2) is pretty well established, two different paths have been proposed for the subsequent proton abstraction (step 3). According to the traditional mechanism **A**, transfer of the proton from C5 of the pyrimidine ring generates a covalently bound enolate intermediate **Int-A**, analogous to the one forming

Scheme 1. (A) Traditional and (B) Proposed Mechanisms of TSase-Catalyzed Reaction

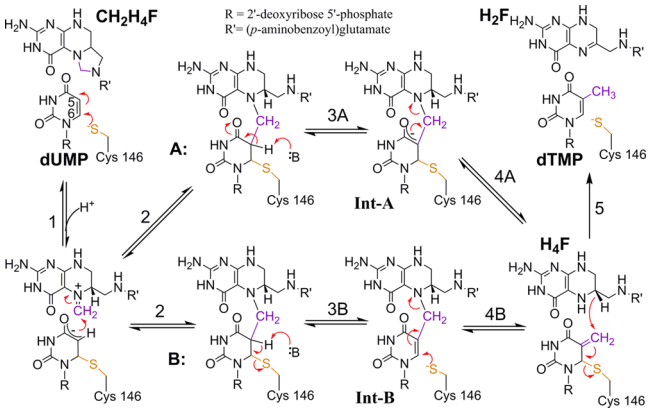

in the solution upon proton exchange at C5 of dUMP in the presence of high concentrations of thiols.[12] In contrast to that, results of QM/MM calculations[8] predicted that the proton abstraction occurs via E_2 with C6−S bond cleavage (step 3B) to form a nonenzyme-bound intermediate **Int-B**. The lability of the S−C bond has independently been supported by structural[13] and binding[14] studies of the mechanism-based inhibitor 5-fluoro dUMP, which forms a reversible covalent ternary complex with CH_2H_4F and TSase, analogous to the intermediate that follows step 2. In path **A**, **Int-A** would lose H_4F (step 4A, Hoffman elimination), while in path **B**, **Int-B** would follow 1−3 SN_2 reaction. Both steps 4A and 4B result in an exocyclic methylene intermediate, which undergoes concerted hydride transfer and C−S cleavage (again 1−3 SN_2 reaction) to form the products.[10,7] The key difference between the traditional path **A** and the calculated path **B** is noncovalently bound nucleotide-folate intermediate **Int-B**. In fact, **Int-B** had been originally considered to be TSase intermediate[15,16] until the discovery of nucleophilic covalent activation of dUMP with active site cysteine and detection of the covalently bound ternary complex in crystal structures.[1] Inspired by that early prediction, several studies reported synthesis and biological activity of stable analogues of **Int-B**, including thyminyl derivatives of H_4F[17,18] and thymidinyl derivatives of dihydro- and tetrahydroquinoline,[19] tetrahydropyridopyrimidines,[20] pyrimidines,[21] tetrahydroquinoxalines,[22] and 8-deaza-5,6,7,8-tetrahydrofolate.[23,24] Interestingly, the latter compound, differing from **Int-B** only at the position 8 of the folate, appeared to be a potent nanomolar competitive inhibitor of human TSase. This intriguing fact and the prediction of QM/

Received: April 13, 2016
Published: June 21, 2016

DOI: 10.1021/jacs.6b03826
J. Am. Chem. Soc. 2016, 138, 8056−8059

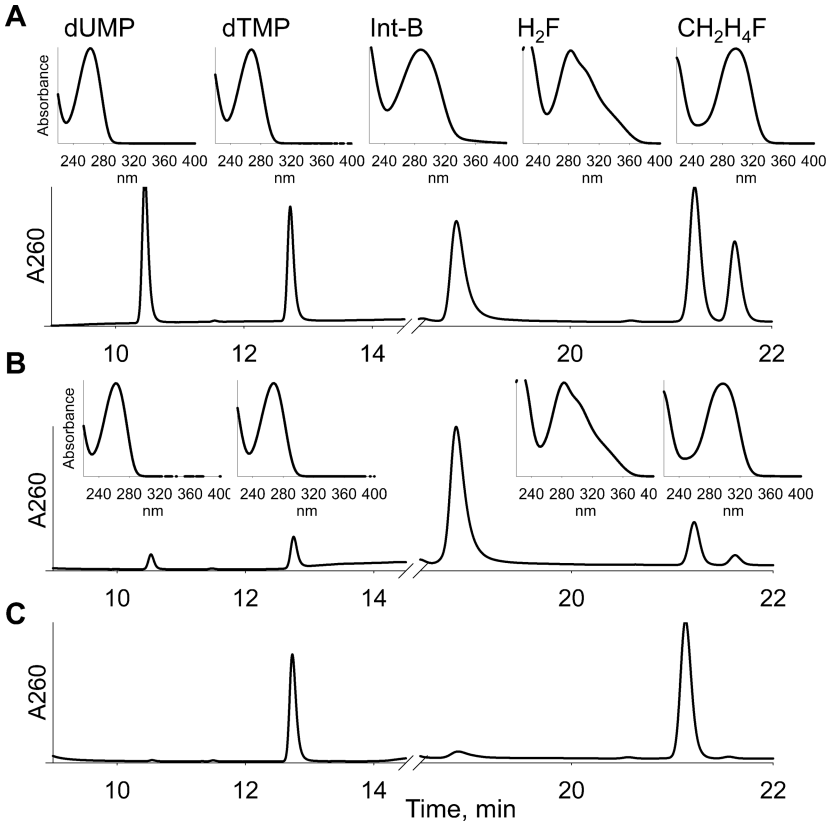

Figure 1. Chromatograms at 260 nm and UV spectra at the peak apexes for: (A) mixture of dUMP, dTMP, Int-B, H_2F, and CH_2H_4F used as standards; (B) **Int-B** after 1 min of incubation in the presence of *Ec*TSase (note the transient formation of substrates dUMP and CH_2H_4F along with products dTMP and H_2F); and (C) **Int-B** after 30 min of incubation in the presence of *Ec*TSase (note the disappearance of transiently formed substrates dUMP and CH_2H_4F as they irreversibly react to form products dTMP and H_2F). Assay conditions: 100 μM **Int-B**, 100 nM *Ec*TSase (dimer), 100 mM Tris-HCl pH 7.5, 50 mM $MgCl_2$, 25 mM DTT, 1 mM EDTA, 7 mM HCHO, 25 °C.

MM calculations encouraged us to examine competence of **Int-B** as an intermediate in the TSase-catalyzed reaction.

Intermediates of enzymatic reactions are often unstable and are not readily accessible in their intact state. To date, only a handful of studies have described either isolation or chemical synthesis of the enzymatic intermediates as well as examination of their chemical and kinetic competence in the corresponding reactions.[25−30] We have synthesized **Int-B** adopting a previously reported strategy for the synthesis of its nonreactive 8-deaza analogue (Scheme S1).[23] However, unlike previous reports we were able to separate individual (6*R*)- and (6*S*)-diastereomers of **Int-B** using C18 HPLC (see Supporting Information, SI). Since only the (6*R*)-CH_2H_4F substrate is active with TSase, only the (6*S*)-diastereomer of **Int-B** is expected to be formed during the TSase-catalyzed reaction illustrated in Scheme 1, path B (note that the stereocenter at C6 of the tetrahydropteridine-ring is the same for (6*R*)-CH_2H_4F and (6*S*)-H_4F or (6*S*)-**Int-B**, and the *S* to *R* change is only due to the nomenclature rules organic chemists follow). To ensure that the correct diastereomer is selected, we employed enzymatic discrimination using *E. coli* TSase (*Ec*TSase). When incubated in the presence of *Ec*TSase, only one of the purified diastereomers of **Int-B** partitioned into products dTMP and H_2F and substrates dUMP and CH_2H_4F (Figure 1, Table 1). This diastereomer was assigned as the intended (6*S*)-**Int-B**, and since the steps preceding the formation of **Int-B** are reversible (Scheme 1), it is expected that dUMP and CH_2H_4F should be generated transiently. Accordingly, transient generation of dUMP and CH_2H_4F was observed as illustrated in Figure 1B. Furthermore, as expected from the fact that step 5 is not reversible, thermodynamically (long reaction times) both **Int-B** and the transiently formed dUMP and CH_2H_4F are fully consumed forming products dTMP and H_2F (Figure 1C). Surprisingly, incubation of the other diastereomer of **Int-B** with *Ec*TSase resulted in a slow formation of CH_2H_4F and DTT-trapped dTMP, which was observed only upon addition of formaldehyde in the reaction mixture (Figure S2). This observation suggests that the enzyme can still bind the (6*R*)-diastereomer of **Int-B** and catalyze its conversion to (6*R*)-H_4F and exocyclic methylene-dUMP (step 4B) leading to dissociation of (6*R*)-H_4F and its chemical trapping by formaldehyde producing (6*S*)-CH_2H_4F, which is accumulated but cannot be consumed by TSase. The remaining exocyclic intermediate was in turn trapped by dithiotreitol (Figure S2; note that reaction of (6*R*)-diastereomer in the reverse direction would result in generation of dUMP and (6*S*)-CH_2H_4F even in the absence of formaldehyde, however dUMP and (6*S*)-CH_2H_4F were not

Table 1. Summary of HPLC and HRMS Analyses of Standards dUMP, dTMP, H_2F, CH_2H_4F, and Int-B and of *Ec*TSase-Generated Products from Conversion of Int-B

	retention time		HRMS *m*/*z* (ESI-) [M − H$^+$]	
sample	standard	TSase generated	calcd	obsd
dUMP	10.45	10.52	307.0331	307.0324
dTMP	12.71	12.76	321.0488	321.0492
H_2F	21.23	21.21	442.1475	442.1475
CH_2H_4F	21.63	21.62	456.1632	456.1616
Int-B	18.87	N/A	764.2041	764.2047

DOI: 10.1021/jacs.6b03826
J. Am. Chem. Soc. 2016, 138, 8056−8059

Scheme 2. Minimal Kinetic Model of *Ec*TSase-Catalyzed Reaction with Microscopic Rate Constants Resulting from Global Fit of the Experimental Data Described in the Text[a]

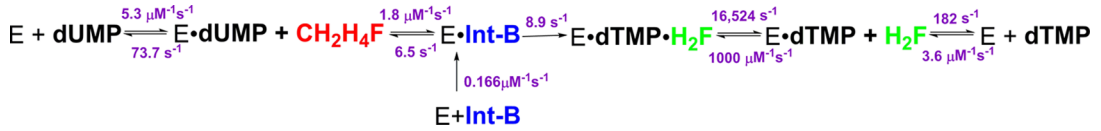

[a]The minimal model has to have a minimum number of steps needed to define the reaction's kinetics. It is obvious that several of the steps involve multiple microscopic steps. For example, the **E·Int-B** conversion to **E**·products (8.9 s^{-1}) involves equilibrium step 4 and irreversible step 5 (Scheme 1) and is the product of the equilibrium and kinetic constants.

detected under the conditions of current experiment). Analogous formation of exocyclic intermediate adducts with thiols has been observed in poorly preorganized mutants of *Es*TSase.[31] In contrast, when formaldehyde was excluded from the reaction mixture containing reactive (6*S*)-diastereomer of **Int-B**, formation of the natural (6*R*)-CH_2H_4F was still observed indicating that its N10N5-methylene originates from **Int-B** as follows from the Scheme 1B. Noteworthy, none of the diastereomers revealed reactivity in the absence of TSase up to 80 min incubation under assay conditions in the absence or presence of formaldehyde. In short, the fact of (6*S*)-**Int-B** but not the (6*R*)-diastereomer partitioning to both products and substrates of the reaction supports its chemical competence as an intermediate of TSase-catalyzed reaction. Thus, further in the text **Int-B** will refer exclusively to (6*S*)-diastereomer of **Int-B**.

To determine the steady-state kinetic parameters for **Int-B** turnover, we have obtained progress curves of **Int-B** enzymatic consumption and CH_2H_4F and H_2F generation at five concentrations of **Int-B** ranging from 23 to 220 μM and globally fit the data to the minimal kinetic model given in the Scheme 2. Figure 2 presents an example of progress curves at [**Int-B**] = 23

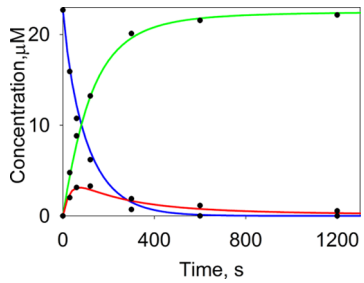

Figure 2. An example of a progress curve of the 23 μM **Int-B** (blue) partitioning into H_2F (green) and CH_2H_4F (red) in the presence of 100 nM *Ec*TSase. Dots represent experimental points and lines that originate from the global fit of the partitioning data as well as to full progress curves for dUMP and CH_2H_4F turnover, to Scheme 2 using KinTek Explorer. A complete set of progress curves can be found in the SI. Each progress curve was reproduced in at least two independent experiments.

μM, and a complete set of progress curves is presented in Figure S1. The invoked model is featuring irreversible binding of **Int-B** and its reversible conversion to CH_2H_4F and dUMP, which can be released from enzyme active site in an ordered fashion. Consequently, formation of products in the forward direction proceeds through direct formation from **Int-B** upon its binding to the enzyme or its reformation from the transiently generated substrates. Clearly, the equilibrium step between **E·dUMP** and **E·Int-B** as well as the following irreversible step are in fact combinations of several chemical and possibly physical steps. However, since experimental data acquired in this work cannot define each individual microscopic step, the kinetic model was simplified. To facilitate the global fit, we have independently measured the kinetics of binding of dUMP and dTMP and included the progress curves for dUMP and CH_2H_4F turnover detected spectrophotometrically at 340 nm (see SI). When fitting the data to the model illustrated in Scheme 2, a good agreement with literature steady-state parameters[32] was found (Table 2). The first-order rate constant for **Int-B** consumption

Table 2. Steady-State Kinetic Parameters of *Ec*TSase-Catalyzed Turnover of dUMP, CH_2H_4F, and Int-B

kinetic parameter	measured[32]	from global fit to Scheme 2
k_{cat}, s^{-1}	8.7 ± 0.2	8.8 ± 0.5
$K_{m,\ dUMP}$, μM	2.4 ± 0.2	3.2 ± 0.1
$K_{m,\ CH2H4F}$, μM	15 ± 1	13 ± 2
$k_{cat}/K_{m,\ CH_2H_4F}$, $\mu M^{-1}\ s^{-1}$	0.58 ± 0.04	0.7 ± 0.1
$k_{cat,Int}$, s^{-1}	N/A	15.1 ± 0.1
$K_{m,Int}$, μM	N/A	100.0 ± 0.1
$k_{cat}/K_{m,Int}$, $\mu M^{-1}\ s^{-1}$	N/A	0.151 ± 0.001

($k_{cat,Int}$) was double that for substrate CH_2H_4F, supporting that **Int-B** is kinetically competent as an intermediate of the *Ec*TSase-catalyzed reaction. Note that $k_{cat,Int}$ is effectively a sum of rate constants for **Int-B** turnover in the forward and reverse direction, consequently it exceeds the rate constant for the products formation. The second-order rate constant ($k_{cat}/K_{m,Int}$) for **Int-B** consumption was almost 5-fold less than that for CH_2H_4F turnover indicating **Int-B**'s slower binding to the enzyme. This result is not surprising considering that in order to prevent excessive stabilization of intermediate, the enzyme has to balance its extremely slow release with slow binding. Note that effectively irreversible binding of transient intermediates allows enzymes to be productive catalysts, as "losing" intermediates during catalytic cycle would not be efficient and is not common at all. Consequently, the dissociation equilibrium constant of an intermediate would be extremely low and effectively zero on the time scale understudy. Binding of intermediates is not a natural path in enzyme evolution, as they are commonly made in the active site, which is consistent with slow binding of an intermediate. Furthermore, the reaction catalyzed by *Ec*TSase is ordered with dUMP binding followed by CH_2H_4F to form a productive Michaelis complex.[33] Consequently, binding of the bisubstrate adduct (**Int-B**) to the predominant conformation of the free TSase in solution is a relatively rare event. Binding of **Int-B** must be accompanied by a slow conformational change of the active site and **Int-B** itself (i.e., "induced-fit"). Attempts to assess the transient-state binding kinetics of **Int-B** were complicated by its reactivity.

In order to distinguish between paths **A** and **B** (Scheme 1), we have globally fit the same data set used to fit Scheme 2 to fit an alternative model (Scheme S2B) in which **Int-B** is irreversibly converted to the substrates dUMP and CH_2H_4F, which in turn

DOI: 10.1021/jacs.6b03826
J. Am. Chem. Soc. 2016, 138, 8056−8059

react forward through **Int-A** to form dTMP and H_2F. Qualitatively, this alternative sequence of events would lead to the same observed outcome as the Scheme 2. However, the alternative fit results in irreversible conversion of the binary **E·dUMP** complex to the **E·Int-A** complex (Table S2). Clearly, this outcome is not consistent with the experimental evidence for the kinetic mechanism of *Ec*TSase-catalyzed reaction and specifically with the fact that hydride transfer is the first irreversible step in the reaction.[34] Consequently, the kinetics of **Int-B** partitioning supports its proposed role as an intermediate of TSase-catalyzed reaction. However, given the experimental and fitting errors, our experimental data do not completely rule out some contribution of pathway **A** or the existence of **Int-A** along the reaction coordinate, if below our detection limit.

In summary, this work provides a critical supporting evidence for the existence of a noncovalently bound nucleotide-folate intermediate (**Int-B**) in the TSase-catalyzed reaction, as predicted by QM/MM calculations. The traditional mechanism suggests the formation of a covalently bound enolate **Int-A** (Scheme 1A). The findings do not distinguish between concerted and stepwise step 4B (Scheme 1). A stepwise 4B means that **Int-B** forms **Int-A** followed by step 4A. Such path is not consistent with the calculations predicting **Int-B**, and at any rate, the important finding is that the mechanism has to involve formation of the noncovalently bound **Int-B**. Several lines of evidence support a concerted rather than stepwise path.

The current findings have both intellectual and practical merits: First, prediction made by QM/MM computations is tested and supported by subsequent experiments, and second, **Int-B** may inspire design of new class of TSase targeting drugs. Although previous attempts to mimic **Int-B** had identified a few potent inhibitors of TSase,[21,23] none of those studies had been followed up. We hope that the current investigation will remind researchers of the possibility of bisubstrate analogues in TSase-targeted drug discovery.

■ ASSOCIATED CONTENT

Supporting Information

The Supporting Information is available free of charge on the ACS Publications website at DOI: 10.1021/jacs.6b03826.

Procedures of the chemical synthesis, enzymatic assays, and data fitting, absorbance progress curves for the TSase-catalyzed reaction, fluorescence binding curves, and NMR spectra (PDF)

■ AUTHOR INFORMATION

Corresponding Author

*amnon-kohen@uiowa.edu

Notes

The authors declare no competing financial interest.

■ ACKNOWLEDGMENTS

This work was supported by NIH Grant R01 GM65368. We thank Ananda Ghosh for expression and purification of *Ec*TSase and Zahidul Islam for preparation of dihydrofolic acid.

■ REFERENCES

(1) Carreras, C. W.; Santi, D. V. *Annu. Rev. Biochem.* **1995**, *64*, 721.
(2) Wilson, P. M.; Danenberg, P. V.; Johnston, P. G.; Lenz, H. J.; Ladner, R. D. *Nat. Rev. Clin. Oncol.* **2014**, *11*, 282.
(3) Costi, M. P.; Gelain, A.; Barlocco, D.; Ghelli, S.; Soragni, F.; Reniero, F.; Rossi, T.; Ruberto, A.; Guillou, C.; Cavazzuti, A.; Casolari, C.; Ferrari, S. *J. Med. Chem.* **2006**, *49*, 5958.
(4) Taddia, L.; D'Arca, D.; Ferrari, S.; Marraccini, C.; Severi, L.; Ponterini, G.; Assaraf, Y. G.; Marverti, G.; Costi, M. P. *Drug Resist. Updates* **2015**, *23*, 20.
(5) Ferrari, S.; Calo, S.; Leone, R.; Luciani, R.; Costantino, L.; Sammak, S.; Di Pisa, F.; Pozzi, C.; Mangani, S.; Costi, M. P. *J. Med. Chem.* **2013**, *56*, 9356.
(6) Salo-Ahen, O. M.; Tochowicz, A.; Pozzi, C.; Cardinale, D.; Ferrari, S.; Boum, Y.; Mangani, S.; Stroud, R. M.; Saxena, P.; Myllykallio, H.; Costi, M. P.; Ponterini, G.; Wade, R. C. *J. Med. Chem.* **2015**, *58*, 3572.
(7) Kanaan, N.; Ferrer, S.; Marti, S.; Garcia-Viloca, M.; Kohen, A.; Moliner, V. *J. Am. Chem. Soc.* **2011**, *133*, 6692.
(8) Wang, Z.; Ferrer, S.; Moliner, V.; Kohen, A. *Biochemistry* **2013**, *52*, 2348.
(9) Kaiyawet, N.; Lonsdale, R.; Rungrotmongkol, T.; Mulholland, A. J.; Hannongbua, S. *J. Chem. Theory Comput.* **2015**, *11*, 713.
(10) Islam, Z.; Strutzenberg, T. S.; Gurevic, I.; Kohen, A. *J. Am. Chem. Soc.* **2014**, *136*, 9850.
(11) Islam, Z.; Strutzenberg, T. S.; Ghosh, A. K.; Kohen, A. *ACS Catal.* **2015**, *5*, 6061.
(12) Wataya, Y.; Hayatsu, H.; Kawazoe, Y. *J. Am. Chem. Soc.* **1972**, *94*, 8927.
(13) Hyatt, D. C.; Maley, F.; Montfort, W. R. *Biochemistry* **1997**, *36*, 4585.
(14) Reilly, R. T.; Barbour, K. W.; Dunlap, R. B.; Berger, F. G. *Mol. Pharmacol.* **1995**, *48*, 72.
(15) Friedkin, M. In *The Kinetics of Cellular Proliferation*; Stohlman, F., Ed.; Grone & Stratton: New York, 1959; p 97.
(16) Huennekens, F. M. *Biochemistry* **1963**, *2*, 151.
(17) Gupta, V. S.; Huennekens, F. M. *Biochemistry* **1967**, *6*, 2168.
(18) Charlton, P. A.; Young, D. W. *J. Chem. Soc., Perkin Trans. 1* **1982**, 1363.
(19) Wilson, R. S.; Mertes, M. P. *Biochemistry* **1973**, *12*, 2879.
(20) Srinivasan, A.; Broom, A. D. *J. Org. Chem.* **1982**, *47*, 4391.
(21) Yang, I. Y.; Slusher, R. M.; Broom, A. D.; Ueda, T.; Cheng, Y. C. *J. Med. Chem.* **1988**, *31*, 2126.
(22) Park, J. S.; Chang, C. T. C.; Mertes, M. P. *J. Med. Chem.* **1979**, *22*, 1134.
(23) Srinivansan, A.; Amarnath, V.; Broom, A. D.; Zou, F. C.; Cheng, Y. C. *J. Med. Chem.* **1984**, *27*, 1710.
(24) Bayomi, S. M. M.; Brixner, D. I.; Eisa, H.; Broom, A. D.; Ueda, T.; Cheng, Y.-C. *Nucleosides Nucleotides* **1988**, *7*, 103.
(25) Cleland, W. W. *Biochemistry* **1990**, *29*, 3194.
(26) Anderson, K. S.; Johnson, K. A. *J. Biol. Chem.* **1990**, *265*, 5567.
(27) Ge, X.; Penney, L. C.; van de Rijn, I.; Tanner, M. E. *Eur. J. Biochem.* **2004**, *271*, 14.
(28) Hawkinson, D. C.; Eames, T. C.; Pollack, R. M. *Biochemistry* **1991**, *30*, 6956.
(29) Hoeffler, J. F.; Tritsch, D.; Grosdemange-Billiard, C.; Rohmer, M. *Eur. J. Biochem.* **2002**, *269*, 4446.
(30) Kholodar, S. A.; Allen, C. L.; Gulick, A. M.; Murkin, A. S. *J. Am. Chem. Soc.* **2015**, *137*, 2748.
(31) Wang, Z.; Abeysinghe, T.; Finer-Moore, J. S.; Stroud, R. M.; Kohen, A. *J. Am. Chem. Soc.* **2012**, *134*, 17722.
(32) Wang, Z.; Sapienza, P. J.; Abeysinghe, T.; Luzum, C.; Lee, A. L.; Finer-Moore, J. S.; Stroud, R. M.; Kohen, A. *J. Am. Chem. Soc.* **2013**, *135*, 7583.
(33) Hong, B.; Maley, F.; Kohen, A. *Biochemistry* **2007**, *46*, 14188.
(34) Spencer, H. T.; Villafranca, J. E.; Appleman, J. R. *Biochemistry* **1997**, *36*, 4212.

DOI: 10.1021/jacs.6b03826
J. Am. Chem. Soc. 2016, 138, 8056−8059